Check for updates

Received: 15 February 2021 | Revised: 15 April 2021 | Accepted: 15 April 2021

DOI: 10.1002/ar.24676

SPECIAL ISSUE ARTICLE

The Anatomical Record | WILEY

Osteology of the enigmatic threadsnake species *Epictia unicolor* and *Trilepida guayaquilensis* (Serpentes, Leptotyphlopidae) with generic insights

Claudia Koch[1] | **Angele Martins**[2,3] | **Mitali Joshi**[1] | **Roberta R. Pinto**[4] | **Paulo Passos**[3]

[1]Zoologisches Forschungsmuseum Alexander Koenig, Bonn, Germany

[2]Departamento de Ciências Fisiológicas, Universidade de Brasília, Brasília, Brazil

[3]Departamento de Vertebrados, Museu Nacional, Universidade Federal do Rio de Janeiro, Rio de Janeiro, Brazil

[4]Laboratório de Diversidade de Anfíbios e Répteis, Museu de Arqueologia e Ciências Naturais da Universidade Católica de Pernambuco, Universidade Católica de Pernambuco, Recife, Brazil

Correspondence
Claudia Koch, Zoologisches Forschungsmuseum Alexander Koenig, Adenauerallee 160, 53113 Bonn, Germany.
Email: c.koch@leibniz-zfmk.de

Abstract

Since the rearrangement of all leptotyphlopid species previously known as "*Leptotyphlops*" in Adalsteinsson et al. (2009)'s paper, several taxa have remained untested regarding their generic identity and have been assigned to different genera based on phenotypic data or, in some cases, without any clear justification. Most of the difficulties in assigning some leptotyphlopid taxa are due to their conserved external morphology, summed with a relatively small number of available specimens, which complicate the recognition of a unique combination of characters for their reasonable generic allocation. On the other hand, recent osteological studies—especially those on the skull—provide relevant data combinations for species assignment and even for the recognition of new genera. In this work, we have attempted to determine the generic allocation of *Epictia unicolor* and *Trilepida guayaquilensis*—both species currently known only by their holotype—based on a detailed description of cranial and post-cranial osteology. We confirm the assignment of *E. unicolor* to the genus *Epictia* despite the divergent configuration of cephalic shields. Based mainly on data from the skull, suspensorium, and cervical vertebrae but supported by external morphology as well as a redescription of the holotype, we propose the assignment of *Trilepida guayaquilensis* to the genus *Epictia*. This study provides not only detailed data on the osteology of *Epictia*, but also a first approach to the putative combination of osteological characters for the genus.

KEYWORDS

burrowing snakes, HRXRT, internal morphology, systematics, taxonomy

This is an open access article under the terms of the Creative Commons Attribution-NonCommercial-NoDerivs License, which permits use and distribution in any medium, provided the original work is properly cited, the use is non-commercial and no modifications or adaptations are made.
© 2021 The Authors. The Anatomical Record published by Wiley Periodicals LLC on behalf of American Association for Anatomy.

1 | INTRODUCTION

The 142 currently recognized species of the fossorial blindsnake family Leptotyphlopidae (Martins et al., 2019; Uetz, Freed & Hosek, 2021) comprise the smallest of all snake species (usually <30 cm in total length) and are among the least studied and poorest known groups of reptiles. Members of the family are widely distributed and inhabit North, Central and South America, Africa, the Arabian Peninsula, and southwest Asia. Previous to the study of Adalsteinsson et al. (2009), all but one species (*Rhinoleptus koniagui*) of the family were placed within the genus *Leptotyphlops* (Orejas-Miranda, Roux-Estève & Guibé, 1970). Adalsteinsson et al. (2009) proposed a new classification by splitting Leptotyphlopidae, which at that time included 116 species, into two subfamilies (Epictinae and Leptotyphlopinae) and 12 genera, based on a hypothesis of phylogenetic relationships obtained from molecular data. For some genera (e.g., *Namibiana*, *Siagonodon*, *Trilepida*) only a single species was genetically analyzed. Thus, due to the lack of molecular data, the assignment of other species to the respective genera was provisionally made based on their belonging to one of 12 previously defined species groups based on external morphological similarities (Broadley, 1999; Broadley & Broadley, 1999; Broadley & Wallach, 1997; Broadley & Wallach, 2007; Hahn, 1978; Orejas-Miranda, 1967; Peters, 1970; Thomas, 1965; Thomas, McDiarmid & Thompson, 1985; Wallach, 1996a; Wallach, 2003; Wallach & Hahn, 1997). However, four species of leptotyphlopids previously assigned to the genera *Rena* and *Siagonodon*, by Adalsteinsson et al. (2009) are now considered to belong to the genus *Trilepida* based on more recent data (Natera Mumaw, Esqueda González & Castelaín, 2015; Pinto & Curcio, 2011; Pinto & Fernandes, 2012; Pinto et al., 2010). Likewise, very recently a species was moved from the genus *Epictia* to a new genus *Habrophallos* (Martins et al., 2019). These newer systematic rearrangements indicate that more detailed studies—mostly combining morphological data—are needed to correctly assign leptotyphlopid species to genera.

Data on skeletal morphology of different species of leptotyphlopids have been accumulated since the 19th century (e.g., Abdeen, Abo-Taira & Zaher, 1991a; Abdeen, Abo-Taira & Zaher, 1991b; Abdeen, Abo-Taira & Zaher, 1991c; Broadley & Broadley, 1999; Broadley & Wallach, 2007; Brock, 1932; Cundall & Irish, 2008; Duerden & Essex, 1923; Duméril & Bibron, 1844; Essex, 1927; Fabrezi, Marcus & Scrocchi, 1985; FitzSimons, 1962; Haas, 1930, 1931, 1959; Hardaway & Williams, 1976; Kley, 2001, 2006; List, 1966; McDowell & Bogert, 1954; Parker & Grandison, 1977; Pinto et al., 2015; Rieppel, 1979; Rieppel, Kley & Maisano, 2009). Broadley and Broadley (1999) studied southern African species of the subfamily Leptotyphlopinae, and found for the first time that the arrangement of the dorsal skull bones (e.g., paired or unpaired parietal; degree of separation in the midline in paired parietals; presence, position and shape of a postparietal bone) provides diagnostic characters that are useful for the differentiation of genera, and in some cases even species. However, skeletal characters have rarely been used to differentiate species and genera (Broadley & Wallach, 2007; Fabrezi et al., 1985), largely because the use of historical dissection methods to visualize the skeleton is extremely difficult in these small snakes. Altogether, information on the skull morphology of 27 African species is available from all four genera of Leptotyphlopinae which share paired nasals, supraoccipitals, otooccipitals, and prootics. Before this special issue, there were only rare exemplar studies of skulls of the subfamily Epictinae (e.g., Martins et al., 2021; Pinto et al., 2015), and only recently have skull characters been used for the first time to define a new genus (*Habrophallos*, see Martins et al., 2019). According to the available information, the species and genera of Epictinae share a fused, unpaired parietal and differ from each other most conspicuously in having paired or unpaired supraoccipital and nasal bones (Broadley, 2004; Cundall & Irish, 2008; Curcio, 2003; Fabrezi et al., 1985; Haas, 1930; Kley, 2006; List, 1966; Martins et al., 2019; McDowell & Bogert, 1954; Pinto et al., 2015; Rieppel et al., 2009; Salazar-Valenzuela et al., 2015).

The species *Trilepida guayaquilensis* (Orejas-Miranda & Peters, 1970; Figure 1), is only known from the holotype (ZMB 4508) (Cisneros-Heredia, 2008; McDiarmid, Campbell & Touré, 1999; Pinto, 2010; Wallach, Williams & Boundy, 2014) and represents one of the species that was generically allocated by Adalsteinsson et al. (2009) merely based on external morphology data provided by Orejas-Miranda and Peters (1970). Pinto et al. (2010) already questioned the generic allocation of *T. guayaquilensis* based on external morphological examination of the holotype, and a recent analysis of the cranial osteology of the genus *Trilepida* (Martins et al., 2021) suggests that the taxon does not belong to this genus.

The species *Epictia unicolor* (Werner, 1913; Figure 2) with uncertain origin (probably from Brazil) and also known only from the holotype (ZMH 8401), was not mentioned in the study of Adalsteinsson et al. (2009), and according to Boundy and Wallach (2008), was also overlooked in earlier studies. Boundy and Wallach (2008) recognized the holotype as a unique species, *Leptotyphlops unicolor*, differing from all known species of the family Leptotyphlopidae by having a subocular scale, a uniform dorsal pattern, fewer than 250 transverse scale rows and a tail length that is <15% of the total length. They further provided a detailed redescription of the holotype and compared it with the other eight leptotyphlopid species known at that time, which share a subocular scale and

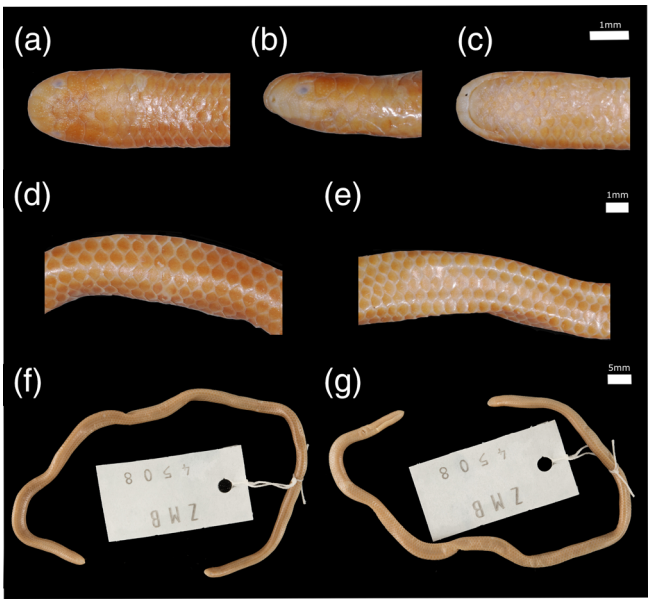

FIGURE 1 Holotype of *Epictia guayaquilensis* (ZMB 4508). (a) Dorsal, (b) lateral, and (c) ventral views of the head. (d) Dorsal and (e) ventral views of the midbody. (f) Dorsal and (g) ventral views of the total body

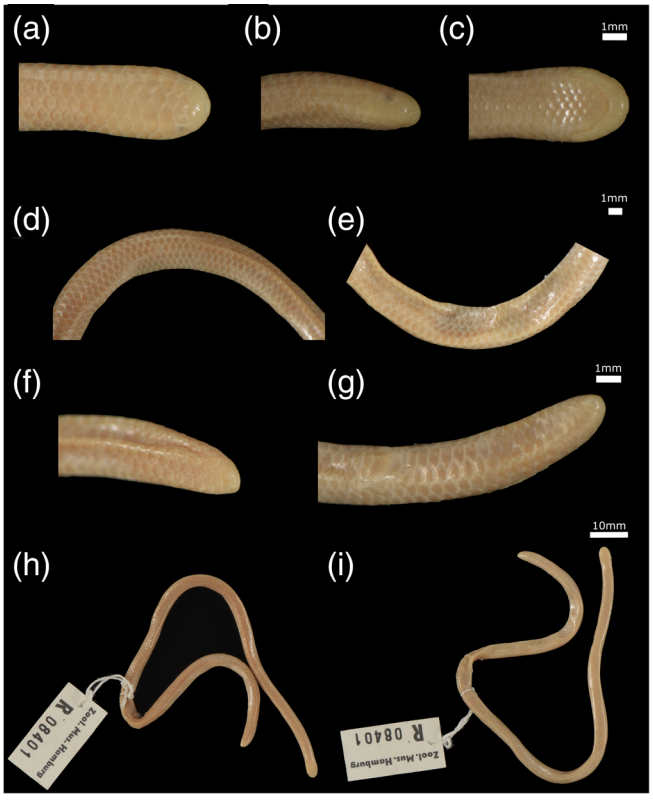

FIGURE 2 Holotype of *Epictia unicolor* (ZMH 8401). (a) Dorsal, (b) lateral, and (c) ventral views of the head. (d) Dorsal and (e) ventral views of the midbody. (f) Dorsal and (g) ventral views of the tail. (h) Dorsal and (i) ventral views of the total body

were assigned by Adalsteinsson et al. (2009) to the New World genera *Mitophis* (*M. asbolepis*, *M. calypso*, *M. leptepileptus*, *M. pyrites*) and *Tetracheilostoma* (*T. bilineata*, *T. breuili*, *T. carlae*), as well as the African genus *Tricheilostoma* (*T. dissimilis*). *Leptotyphlops unicolor* was later assigned to the genus *Epictia* by Wallach et al. (2014) without any justification.

In order to better assess the taxonomic status of *Epictia unicolor* and *Trilepida guayaquilensis*, we examined their holotypes and obtained high-resolution x-ray computed tomography (HRXCT) images that allowed us to provide detailed osteological descriptions. Since skull morphology data has proven to be very conserved intragenerically and is therefore useful for the systematics of leptotyphlopids (but see Martins et al., 2019; Martins et al., 2021), we propose the assignment of both species to the genus *Epictia* based on osteological data and provide a redescription of the holotype of *Trilepida guayaquilensis*.

2 | MATERIALS AND METHODS

We obtained X-ray images of the head, upper body and the cloacal region of the holotypes of *Epictia unicolor* (ZMH 8401) and *Trilepida guayaquilensis* (ZMB 4508) in three dimensions (3D) using a high-resolution micro-CT scanner (Bruker SkyScan 1173) at the Zoologisches Forschungsmuseum Alexander Koenig (ZFMK) in Bonn, Germany. We used the following settings: an X-ray beam with 35–38 kV source voltage and 114–160 μA current, no filter, rotation steps of 0.25°–0.3°, frame averaging of 5, 180° rotation, resulting in 800–960 projections of 500–600 ms exposure time each and a total scan duration of 56 min. The magnification setup generated data with an isotropic voxel size of 6.4–7.1 μm. The CT-datasets were reconstructed using N-Recon software (Bruker MicroCT). Amira visualisation software (FEI, Thermo Fisher Scientific) was used to render and segment the datasets of the skulls in 3D, and images were created showing each bone in a different color. Terminology for anatomical structures follows List (1966), Rieppel (1979), Cundall and Irish (2008), Rieppel et al. (2009), Martins (2016), and Martins et al. (2021) for the skull; Kley (2006), Martins (2016), and Martins et al. (2021) for the suspensorium; Romer (1956), List (1966), Holman (2000), and Martins et al. (2021) for the cervical vertebrae; and List (1966) and Martins et al. (2021) for the pelvic girdle. For the redescription of the holotype of *T. guayaquilensis*, measurements were taken with a dial caliper to the nearest 0.1 mm, except for total length (TL) and tail length (TAL), both of which were taken with a graduated ruler to the nearest 1.0 mm. External morphology follows Pinto and Curcio (2011).

3 | RESULTS

The presence of paired supraoccipital bones distinguishes both species from species of all New World genera of Leptotyphlopidae except *Epictia* and *Rena*. In contrast to species of the genus *Rena* and consistent with species of the genus *Epictia*, the otooccipitals are in ventral contact and exclude the basioccipital from participating in the formation of the foramen magnum. Based on these conditions, both species are thus assigned to the genus *Epictia*.

3.1 | Skull of *Epictia guayaquilensis* (new combination) and *E. unicolor* (Figures 3–5)

The premaxilla is roughly semicircular (*E. guayaquilensis*; Figure 4c) or pentagonal (*E. unicolor*; Figure 4a) with concave lateral margins in anterior view, and about pentagonal or trapezoidal (*E. unicolor*; Figure 3c) in ventral view. This bone is edentulous and pierced by five foramina (in *E. guayaquilensis* two in anterior view (Figure 4c) and three in ventral view (Figure 3f); in *E. unicolor* one in anterior view (Figure 4a) and four in ventral view (Figure 3c). These foramina most likely give path to the rami of the *ophthalmicus profundus* nerve (V1; Haas, 1964). The premaxilla contacts the nasals dorsally, the vomers ventroposteriorly, the maxillae ventrolaterally, and the septomaxillae ventrolaterally and posteromedially (Figures 3b,c,e,f, 4a,c, and 5a,e). In anterior view the premaxilla shows a finger-like dorsally projecting expansion (Figure 4a–c) that ends dorsally just before reaching the lower level of the nasals, and which is the only visible part of the premaxilla in dorsal view (Figure 3a,d). An internasal and transverse process are absent and the vomerine process is short, tapered and single in *E. guayaquilensis* (Figure 3f) and double in *E. unicolor* (Figure 3c). The premaxilla has an internal medial septum that supports the *septum nasi* dorsally and contacts the septomaxillae posteromedially (internally; Figure 5a,e).

The **nasals** are paired, approximately rectangular and about twice longer than wide in dorsal view (Figure 3a, d). In *E. guayaquilensis*, each nasal is pierced by two foramina (Figure 3d), one situated in the central region of the bone and the other close to the posterolateral corner near the suture with the frontal and prefrontal, the

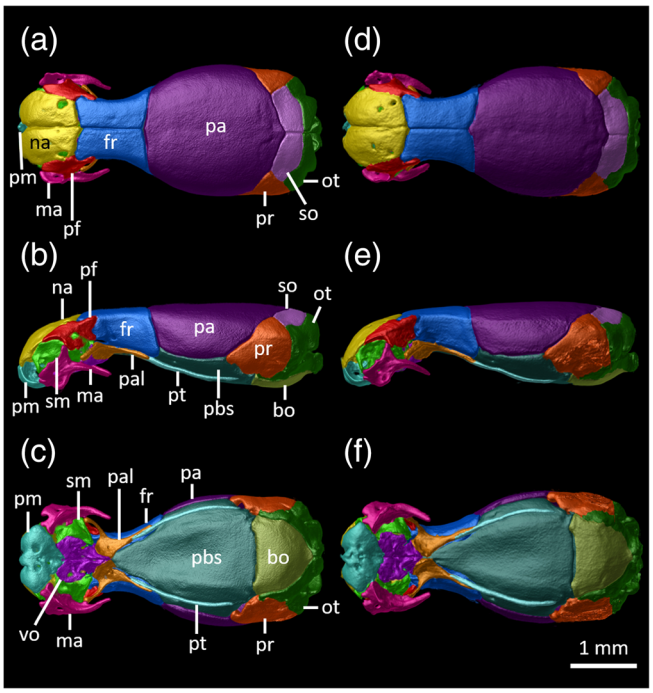

FIGURE 3 (a,d) Dorsal, (b,e) lateral, and (c,f) ventral views of the skull of the holotypes of *Epictia unicolor* (a–c, ZMH 8401) and *E. guayaquilensis* (d–f, ZMB 4508) based on µCT data. Different skull elements were digitally colored and the mandible and quadrates were removed for better visualization. bo, basioccipital; fr, frontal; ma, maxilla; na, nasal; ot, otooccipital; pa, parietal; pal, palatine; pbs, parabasisphenoid; pf, prefrontal; pm, premaxilla; pr, prootic; pt, pterygoid; sm, septomaxilla; so, supraoccipital; vo, vomer

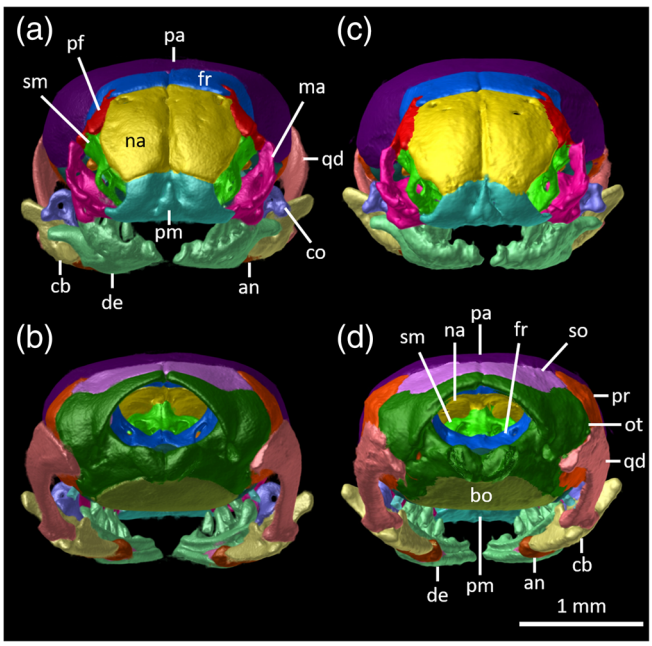

FIGURE 4 (a,c) Anterior and (b,d) posterior views of the skull and lower jaw of the holotypes of *Epictia unicolor* (a,b, ZMH 8401) and *E. guayaquilensis* (c,d, ZMB 4508) based on µCT data. Different skull elements were digitally colored to improve visualization. an, angular; bo, basioccipital; cb, compound bone; co, coronoid; de, dentary; fr, frontal; ma, maxilla; na, nasal; ot, otooccipital; pa, parietal; pf, prefrontal; pm, premaxilla; pr, prootic; qd, quadrate; sm, septomaxilla; so, supraoccipital

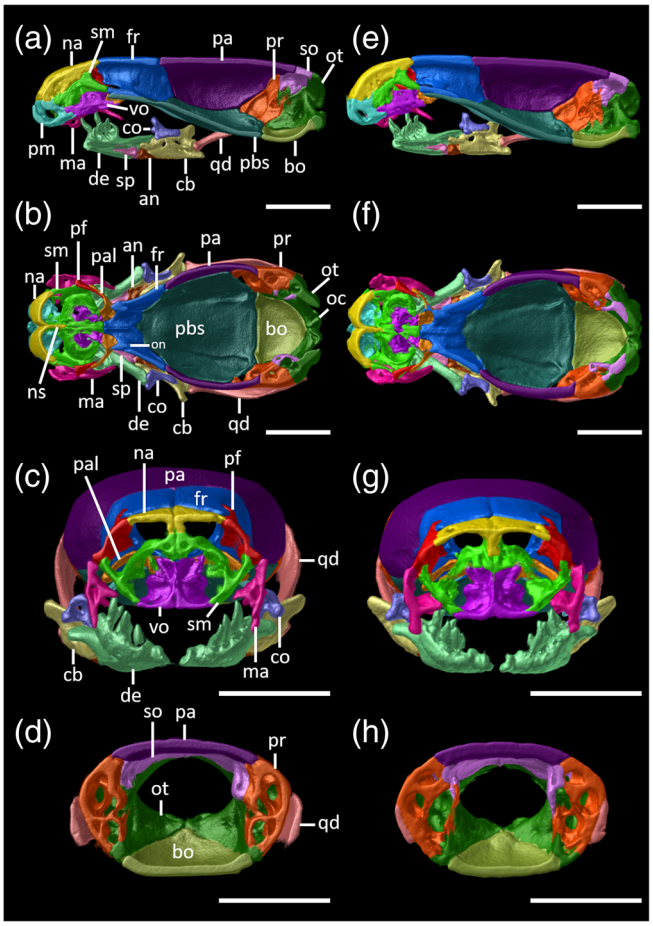

FIGURE 5 Three-dimensional cutaway views along the (a,e) sagittal, (b,f) vertical, and (c,d,g,h) transverse axes of the skulls of the holotypes of *Epictia unicolor* (a–d, ZMH 8401) and *E. guayaquilensis* (e–h, ZMB 4508) based on μCT data. Different skull elements were digitally colored to improve visualization. an, angular; bo, basioccipital; cb, compound bone; co, coronoid; de, dentary; fr, frontal; ma, maxilla; na, nasal; ns, nasal septum; oc, occipital condyle; on, optic nerve foramen; ot, otooccipital; pa, parietal; pal, palatine; pbs, parabasisphenoid; pf, prefrontal; pm, premaxilla; pr, prootic; qd, quadrate; sm, septomaxilla; so, supraoccipital; sp, splenial; vo, vomer. Scales: 1 mm

latter most likely representing the *apicalis nasi* nerve foramen. In *E. unicolor*, each nasal is also pierced by two foramina (Figure 3a), but the posteromedial ones are wide and laterally enclosed by the prefrontal, while the medial ones are reduced and located at the suture between both nasals. Each nasal contacts the premaxilla anteriorly and anteroventrally, the frontal posteriorly, the prefrontal lateroposteriorly, and the septomaxillae lateroanteriorly and medially (Figures 3a,b,d,e, 4a,c, and 5a–c,e–g). The anterior contact with the premaxilla (Figure 4a,c) and posterior contact with the frontals (Figure 3a,d) are oblique. The dorsal surface of the nasals is convex (Figures 3a,b,d,e, 4a,c, and 5a–c,e–g), with each element projecting midventrally to form the paired nasal septum (internally; Figure 5a–c,e–g) that is ventrally supported by the short medial lamina of the premaxilla anteriorly (Figure 5a,e) and by the septomaxilla posteriorly (Figure 5a–c,e–g).

The **prefrontals** are paired, subtriangular in dorsal view (Figure 3a,d) and irregularly shaped in lateral view (Figure 3b,e), located lateral to the snout complex. Each prefrontal tapers to contact the nasal anteromedially (anterior process; Figure 3a,–b,d,e), the frontal posteromedially (Figure 3a,d) and posteriorly (frontal process; Figure 3b,e), the septomaxilla ventrally (Figures 3b,e and 5c,g), and the dorsal tip of the maxilla lateroventrally (maxillary process; Figures 3b,e, 4a,c, and 5c,g). The recess formed by the descending maxillary process is anteroventrally oriented (Figure 3b,e).

The **septomaxillae** are paired, complex in shape, not visible and covered by the nasals and frontal in dorsal view, partly visible in anterior (Figure 4a,c), lateral (Figure 3b,e) and ventral views (Figure 4c,f). Each septomaxilla contacts the nasal dorsally (Figure 5a,e) and dorsolaterally (Figure 3b,e), the premaxilla anteroventrally (Figure 5a,e), the vomer ventrally (Figure 5a,e), the maxilla laterally (Figure 4a,c), the prefrontal dorsolaterally (Figures 3b,e and 5c,g), and the midventral region of the frontal posteriorly (Figure 5a,b, e,f). Posteriorly it approaches the palatine but remains marginally separated from it (Figure 3c,f). Each septomaxilla expands dorsolaterally to form an ascending process that slightly inflects medially and contacts the prefrontal and nasal dorsally and the maxilla laterally (Figures 4a,c and 5b,c,f,g), although the latter contact is only marginal in *E. unicolor* (Figure 5c). In *E. guayaquilensis*, the ascending process seems to be perforated by at least two large foramina (Figures 3e and 4c). However, it is difficult to determine the exact structure and number of foramina, as the septomaxilla in the CT images shows strong density differences in the bone material, so that it is not always possible to clearly determine whether the septomaxilla is extremely thin or perforated at a certain area. In *E. unicolor*, the ascending process of the septomaxilla is perforated by a wide anterior foramen, and the right septomaxilla additionally has a reduced foramen located ventral to the former (Figures 3b and 4a). Medially (internally), each septomaxilla develops a wide lamina that forms the dorsal cover of the vomeronasal cupola (Figure 5a–c,e–g). This lamina expands dorsoposteriorly, inflecting medially to form, together with the subolfactory process of the frontal, the passage for the vomeronasal nerve (Figure 5a, b,ef). The dorsal (= internal) lamina of the septomaxilla contacts the premaxilla anteriorly (Figure 5a,e) and the nasal septum posteriorly (Figure 5a,c,e,g). The dorsal

surface of this internal lamina is grooved by the sulcus for the medial *ophthalmicus profundus* nerve (Figure 5b, c,f,g).

The **vomers** are paired, in firm medial contact along their entire length and visible in ventral view where together they are roughly heart-shaped (Figure 3c,f), located midventral to the vomeronasal cupola (Figure 5c, g). Each vomer contacts the premaxilla anteriorly (Figure 3c,f), septomaxilla dorsally (Figure 5a,c,e,g) and palatine posteriorly (Figure 3c,f). Posteriorly the vomer is slightly separated from the anterior tip of the parabasisphenoid rostrum and it seems to be slightly separated from the ventral region of the frontal (which lies dorsally above the palatine; Figure 5a,e), however this condition is difficult to see in the reconstructed CT images as the exact position of the suture between vomer and palatine is not clearly visible in dorsal view. Each vomer is pierced by an oval to slit-like foramen in its ventral lamina (Figure 3c,f). The anterior limit of the vomers is partially covered by the vomerine process of the premaxilla (Figure 3c,f). The lateral wing of each vomer is wide (Figure 3c,f), exhibiting a short posterior process that bends dorsally (Figure 5c,g). The posterior processes of the vomers are in medial contact with each other along their entire length and with the palatine posterolaterally (Figure 3c,f). Each posterior process also bears a very short ventral process.

The **frontals** are paired, nearly trapezoidal in dorsal view, about twice as long as broad (Figure 3a,d). The anterior, posterior and medial margins are approximately straight and the lateral margins concave (Figure 3a,d). Each frontal contacts anteriorly the posterior margin of the nasal, anterolaterally the prefrontal, posteriorly the anterior margin of the parietal (Figure 3a,d), ventrally the palatine, parabasisphenoid and pterygoid (Figure 3b, c,e,f), and anteroventrally the posteromedial region of the septomaxilla (Figure 5a,b,e,f). The lateral surface of the frontal is slightly concave, being pierced by the anteroposteriorly oriented optic nerve foramen (Figure 3b,e), the anterior opening of which is visible in anterior view on the ventral lamina of the frontal, while the posterior opening is visible in posterior view dorsally on the ventral lamina (Figures 4b,d and 5b,f). Each frontal descends laterally (Figure 3b,e) and inflects medially to contact its counterpart (internally) dorsal to the parabasisphenoid to form the frontal subolfactory process (Figures 4b,d and 5b,f).

The **maxillae** are edentulous, irregular in shape, pierced by two (right maxilla of *E. guayaquilensis* and both of *E. unicolor*) or three (left maxilla of *E. guayaquilensis*) foramina in lateral view (Figure 3b,e). Each maxilla has three processes: a lateral process that inflects dorsally and abuts the prefrontal via a dorsal triangular process that might (left maxilla of *E. guayaquilensis*) or might not (right maxilla of *E. guayaquilensis* and both of *E. unicolor*) bear a foramen at its base; a comparatively small dentigerous process that is pierced by a foramen; and a long, rod-like and posteriorly slightly tapered posterior process that inflects ventromedially and is slightly dorsoventrally compressed and does not bear any foramen (Figure 3b,e). Each maxilla contacts (*E. guayaquilensis*; Figure 3c) or not (*E. unicolor*; Figure 3f) the premaxilla anteriorly, the septomaxilla medially (Figure 3c,f), and with the dorsal tip of the lateral process the prefrontal dorsally (Figure 3b,e). In both species, the lateral process is undeveloped and laterally exposes almost all of the ascending process of the septomaxilla (Figure 3b,e). In *E. guayaquilensis*, the posterior process of the left maxilla contacts the anterior tip of the maxillary process of the left palatine (Figure 3e), while in *E. unicolor* both elements do not seem to be in contact (Figure 3b).

The **parietal** is single, wide, roundish in dorsal view, representing the largest and broadest bone of the braincase (Figure 3a,d). It contacts the frontals anteriorly (Figure 3a,d), the supraoccipitals posteriorly (Figure 3a, d), the prootics posteroventrally (Figure 3a,b,d,e), and the parabasisphenoid ventrally (Figure 3b,C,e,f). Its posteromedial dorsal surface exhibits inconspicuous concavities in *E. unicolor* (Figure 3a) that possibly provide attachment areas for tendons of neck muscles (see Martins, Passos, & Pinto, 2019). In *E. guayaquilensis* its medial anterior limit projects into a tapered, short process that separates both frontals in their posterior limit (Figure 3d); this process is absent in *E. unicolor*, in which the parietal forms an approximately straight suture with the frontals (Figure 3a). The lateral walls are convex and the posterior suture of the parietal with each supraoccipital is oblique and almost straight (Figure 3a, d). The parietal is not pierced by a foramen nor is it involved in the formation of the trigeminal nerve foramen, and internal pillars (sensu Martins et al., 2021) are absent (Figure 5a,e).

The **parabasisphenoid complex** is roundish with an arrow-like shape, tapered at its anterior portion (parasphenoid rostrum; Figure 3b,c,e,f). It contacts the frontals anteriorly (Figure 3c,f) and dorsal to the parasphenoid rostrum (Figure 5a,b,e,f), the palatines anterolaterally (Figure 3b,c,e,f), the parietal and the prootics dorsolaterally Figure 3b,c,e,f), the basioccipital posteriorly (Figure 3c,f), and a small portion of the pterygoids ventrally (Figure 3b,c,e,f). The lateral edges are bent dorsolaterally, so that the parabasisphenoid is also partly visible in lateral view Figure 3b,e). Its posterior suture with the basioccipital is about straight along most of its length, except for the presence of lateral concavities

(Figure 3c,f). The wide and oval trigeminal nerve foramen is formed on each side at the suture of the parabasisphenoid with the prootic (Figure 3c,f). Internally, the parabasisphenoid complex is perforated by the foramen of the parabasal canal, located anterolaterally (Figure 5b,f). The dorsoposterior (internal) surface of the parabasisphenoid is pierced by the wide facial nerve palatine branch foramen (visible externally in *E. unicolor*), and by the reduced and almost imperceptible cerebral carotid foramen, which is located posterior to the former (Figure 5b,f).

The **basioccipital** is single and bell-shaped in ventral view (Figure 3c,f). The widest part of the bone is at its anterior suture with the parabasisphenoid and is wider than the basioccipital is long, posteriorly the basioccipital gradually tapers to its blunt end (Figure 3c,f). It contacts the parabasisphenoid anteriorly, the prootics anterolaterally, and the otooccipitals laterally and posteriorly (Figure 3c,f). The basioccipital is not pierced by any foramen and does not participate in the formation of the foramen magnum due to a ventral contact of the otooccipitals (Figures 3c,f, 4b,c, and 5b,d,f,h).

The **supraoccipitals** are paired, wider than long, roughly rectangular in dorsal view, but with a concavity at their posterolateral edge (Figure 3a,d), which is more conspicuous in *E. guayaquilensis* (Figure 3d). Each supraoccipital contacts the parietal anteriorly (Figure 3a, d), the prootics laterally (Figure 3a,d) and lateroventrally (internally; Figure 5a,d,e,h), and the otooccipitals posteriorly (Figure 3a,d). The supraoccipitals do not participate in the formation of the foramen magnum (Figure 3a,d). The medial (internal) wall is perforated by the wide endolymphatic foramen (Figure 5a,e).

The **prootics** are paired and irregularly shaped in lateral view (Figure 3b,e). Each prootic contacts the parietal anteriorly and anterodorsally (Figure 3b,e), the supraoccipital posterodorsally (Figure 3a,b,d,e), the otooccipital posteriorly (Figure 3b,e) and ventrally (Figure 3c,f), the basioccipital at a short anteroventral region (Figure 3c,f), and the parabasisphenoid anteroventrally (Figure 3b,c,e,f). The medial (internal) wall of each prootic is irregular and pierced by a pair of distinct acoustic nerve foramina (Figure 5a,e). A statolythic mass in the otic capsule is absent and a stapedial footplate is apparently not co-ossified with the prootic (Figure 5d,h).

The **otooccipitals** are paired, wide and irregular shaped, visible in dorsal, lateral, ventral and posterior views (Figures 3 and 4b,d), and form the posterior portion of the otic capsule (Figure 5a,b,e,f). Each otooccipital descends laterally and inflects medially to contact its counterpart ventrally thereby excluding the basioccipital from the foramen magnum and forming a short but distinct atlantal process (sensu Cundall & Irish, 2008; Figures 3c,f and 4b,d). The otooccipitals contact the supraoccipitals anterodorsally (Figure 3a,d), the prootics anterolaterally (Figure 3b,e), and the basioccipital ventrally (Figure 3c,f). In posterior view, slightly posterior to the quadrate, each otooccipital bears a wide vagus nerve foramen and a small foramen located medially to the former (Figure 4b,d). The medial (internal) surface of the otooccipitals is irregularly shaped and pierced by a foramen that opens in the juxtastapedial recess, and possibly represents the perilymphatic foramen (Figure 5a,e).

The **palatines** are paired and triradiate, visible in ventral view, and slightly separated from each other medially (Figure 3c,f). Each palatine contacts the vomer anteriorly (Figure 3c,f), the frontal dorsally (Figure 3b,e), the parabasisphenoid rostrum anterodorsally (Figure 3c, f) and the anterior fifth of the pterygoid posteromedially (Figure 3c,f). The palatine is composed of three processes: the long and thin, anterolaterally oriented maxillary process, that approaches and contacts (left palatine) or not (right palatine) the maxilla (Figure 3c,f); the short and broad, medial and dorsoventrally flattened choanal process that inflects ventrally to contact the posterior process of the vomer, also being pierced by a very reduced foramen (Figure 3b,c,e,f); and the long and thin, posteriorly oriented pterygoid process, that medially abuts to the anterior region of the pterygoid (Figure 3c,f).

The **pterygoids** are slender and rod-like, entirely visible in ventral view (Figure 3c,f) and partially visible in lateral view (Figure 3b,e), not contacting the quadrates posteriorly, and not reaching the posterior end of the parabasisphenoid, ending at the level of the trigeminal nerve foramen (Figure 3b,c,e,f). Each pterygoid contacts anteriorly the pterygoid process of the palatine laterally (Figure 3c,f) and the frontal dorsally (Figure 3c,f). At about mid-length, the pterygoid touches the parabasisphenoid over a short section dorsally, whereas throughout the rest of its length it comes very close to the parabasisphenoid, but without touching it (Figure 3b,e). Each pterygoid is almost straight in the anterior half and slightly bends medially throughout its posterior half (Figure 3c,f). An ectopterygoid is indistinct or absent.

3.2 | Suspensorium and mandible of *Epictia guayaquilensis* and *E. unicolor* (Figure 6)

The **lower jaw** is suspended from the skull by a pair of long and slender quadrates. The quadrates have a slightly greater length compared to the length of the entire mandible. Each **quadrate** is connected to the skull by a series of muscles and ligaments (Kley, 2006; Martins, Passos &

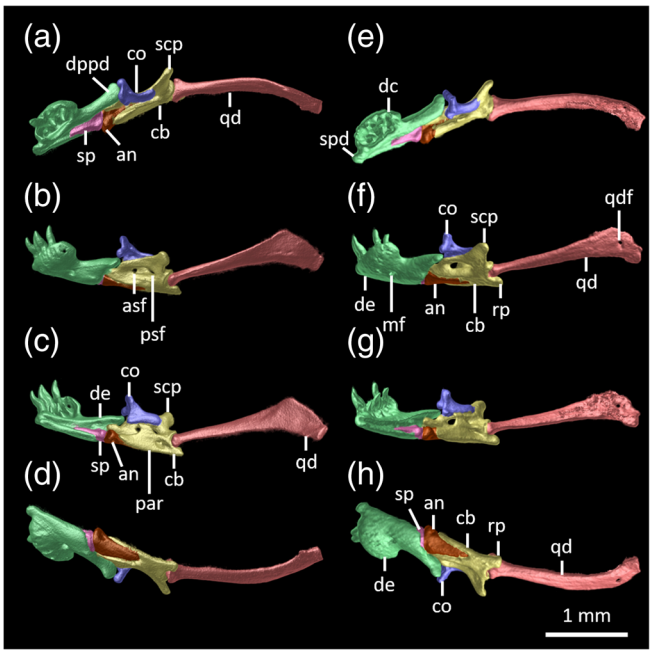

FIGURE 6 (a,e) Dorsal, (b,f) lateral, (c,g) medial, and (d,h) ventral views of the three-dimensional reconstruction of the suspensorium of the holotypes of *Epictia unicolor* (a–d, ZMH 8401) and *E. guayaquilensis* (e–h, ZMB 4508) based on μCT data. Different skull elements were digitally colored to improve visualization. an, angular; asf, anterior surangular foramen; cb, compound bone; co, coronoid; dc, dental concha; de, dentary; dppd, dorsoposterior process of dentary; mf, mental foramen; par, prearticular lamina of compound bone; psf, posterior surangular foramen; qd, quadrate; qdf, quadrate foramen; rp, retroarticular process; scp, supracotylar process of surangular; sp, splenial; spd, symphyseal process of dentary

Pinto, 2019) at the level of the otic capsule, contacting medially the prootic along its entire length and the anterolateral region of the otooccipital. At this contact region, the quadrate is laterally compressed, several times wider than its distal epiphysis, and pierced by a very reduced foramen (apparently absent in *E. unicolor*; Figure 6b,c) located approximately centrally on the flattened surface of the bone (Figure 6f,g). The proximal head of the quadrate also bears a well-developed quadrangular posterior process that develops posterior to the quadrate foramen. The quadrate twists distally along its own axis, becoming progressively slenderer and angling medially towards its distal head, where it articulates with the posterior region of the compound bone to form the quadratomandibular joint (Figure 6a,e).

The **mandible** is short, and composed of the dentary, splenial, angular, coronoid, and compound bone. The **dentary** represents the most distal bone of the mandible, contacting the splenial medially (Figure 6a,c,e,g), and the angular and compound bone posteriorly (Figure 6b,c,f,g). The symphyseal process corresponds to a reduced anteromedial projection of body, projecting beyond the anterior margin of the dental concha (Figure 6a,e). The dental concha exhibits a series of five slightly curved teeth with pleurodont implantation lacking a medial support, ankylosed to the inner surface of the anterolateral margin of the dental concha (Figure 6c,g). A mental foramen is located at the lateral surface of the body of dentary, at about the level of the penultimate and last teeth (Figure 6b,d,f,h). The posteromedial portion of the body of dentary supports most of the splenial, covering it almost completely in lateral view (Figure 6b,f). The dorsoposterior process of the dentary is long and projects towards the dorsal process of the coronoid, reaching the level of the anterior limit of the coronoid (Figure 6a,e).

The **splenial** is the smallest bone of the lower jaw, triangular, tapering anteriorly to reach to the level of the fourth/fifth tooth (Figure 6a,c,e,g). It is hardly visible in lateral view (Figure 6b,f), being attached to the medial surface of the body of dentary (Figure 6a,c,e,g). It contacts the dentary laterally and the angular posteriorly (Figure 6a,c,e,g). An anterior mylohyoid foramen is absent.

The **angular** resembles the splenial in shape, although it tapers posteriorly to almost reach (*E. guayaquilensis*; Figure 6f) the posterior limit of the posterior surangular foramen or it reaches to about the level of the center of the fused anterior+posterior surangular foramina (*E. unicolor*; Figure 6b). The angular contacts the splenial and dentary anteriorly, and the compound bone, dorsally, posteriorly and medially. It runs mainly along the ventral side of the compound bone and is therefore visible mainly from the ventral (Figure 6d,h) and lateral (Figure 6b,f) views. In medial view, the prearticular lamina of the compound bone covers the anterior process of the angular; therefore, the cotylar head of the angular is significantly exposed (Figure 6c,g). The posterior mylohyoid foramen is positioned on the ventromedial surface of the angular (Figure 6d,h).

The **coronoid** is complex in shape, located dorsomedially to and in firm contact with the compound bone (Figure 6c,g), where it extends approximately from the anterior margin of the anterior surangular foramen to behind the posterior margin of the posterior surangular foramen (*E. guayaquilensis*; Figure 6g), or from the anterior to posterior limits of the fused foramina in *E. unicolor* (Figure 6c). Its dorsal process consists of three short projections (lateral, medial and dorsal) in *E. guayaquilensis*, giving the dorsal process a duckfoot-shaped form (Figure 4c). In *E. unicolor*, however, the dorsal process lacks the dorsal projection (Figure 4a). In *E. guayaquilensis*, the medial and dorsal projections are similar in length, whereas the lateral projection is slightly

longer (Figure 4c); while in *E. unicolor* both lateral and medial projections are equal in size (Figure 4a). The anterior surface of the dorsal process is concave with a small anteroposteriorly oriented foramen in its center (Figures 4a and 6c,g), which is also visible at its posterior convex surface (Figures 4b and 6b,f).

The **compound bone** is a complex structure, representing the fusion of the articular, prearticular, and surangular. In lateral view, the anterior process of the surangular portion is partially occluded by the dorsoposterior process of the dentary (Figure 6b,f). The surangular portion expands posteriorly to form the dorsolaterally oriented supracotylar process, which projects dorsally as far as the dorsal process of the coronoid (Figure 6a,b,e,f). The area between the anterior and supracotylar processes of the surangular portion is pierced by an anterior and a posterior foramen (Figure 6b,c,f,g), which can also be merged to a single foramen (right mandible of *E. guayaquilensis* and both of *E. unicolor*; Figure 6b). When distinct, both foramina are located slightly below the coronoid, so that the latter does not participate in the formation of the foramina (Figure 6b,c,f,g). The anterior foramen is located below the anterior limit of the coronoid and the posterior foramen is located slightly anterior to the posterior limit of the coronoid (Figure 6c,g). The prearticular portion of the compound bone is mostly visible in medial view, and tapers slightly anteriorly, where it ends bluntly at the suture with the angular, not reaching the anterior limit of the surangular portion (Figure 6c,g). The prearticular portion has a freely extending dorsal process that reaches over the surangular foramina to the level of the lower edge of the coronoid, but without touching the coronoid or the dorsal border of the foramina (Figure 6c,g). The articular portion of the compound bone is concave posteriorly and forms the articular cotyle of the quadratomandibular joint, ventral to which lies a short retroarticular process, extending posteriorly and slightly curving medially (Figure 6b–d,f–h). In lateral view, this process protrudes posteriorly slightly beyond the level of the supracotylar process of the compound bone (Figure 6b, f). The portion anterior to the retroarticular process is pierced by the *chorda tympani* of the hyomandibular ramus of the facial nerve (VII), which is wide in *E. unicolor* (Figure 6c) and reduced in *E. guayaquilensis* (Figure 6g).

3.3 | Cervical vertebrae of *Epictia guayaquilensis* and *E. unicolor* (Figures 7 and 8)

The **atlas** (Figure 7) is the first cervical vertebra and articulates with the occipital condyle. It is roughly rounded (Figure 7a,d,f,i), composed of paired neural arches that are

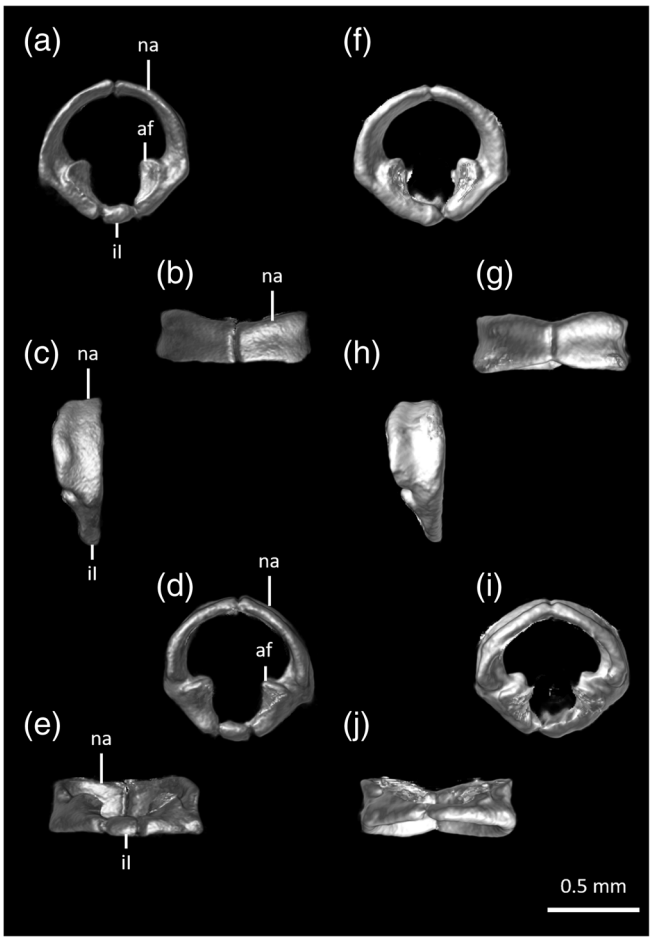

FIGURE 7 Three-dimensional reconstruction of the atlas of the holotypes of *Epictia unicolor* (a–e, ZMH 8401) and *E. guayaquilensis* (f–j, ZMB 4508) in (a,f) anterior, (b,g) dorsal, (c,h) lateral, (d,i) posterior and (e,j) ventral views. af, articular facet; iI, intercentrum I; na, neural arches

fused dorsally (Figure 7g) and ventrally (Figure 7i) in *E. guayaquilensis*. It lacks the ventral intercentrum I, neural spine and ribs. In *E. unicolor*, a distinct and approximately ellipsoidal intercentrum I seems to be laterally fused with the neural arches (Figure 7d,e). The neural arches are significantly broader dorsally (Figure 7b,g) and laterally (Figure 7c,h) than ventrally (Figure 7e,j). Midventrally the neural arches form articular facets (Figure 7a,d,f,i), which articulate with the occipital condyle of the skull. They are slightly notched in the middle along their dorsal and lateral extensions, resulting in a concave surface (Figure 7a,d,f,i). The atlas bears short lateral projections (Figure 7a,d,f,i).

The **axis** (Figure 8) represents the second cervical vertebra and articulates with the posterior face of the atlas. It lacks ribs and is a completely fused element, composed of a centrum, moderate neural arches, an little developed spinal process, an odontoid process, a dorsoanterior process of the odontoid, a pair of undeveloped transverse

processes, postzygapophyseal articular facets, a condyle and reduced intercentra II and III (Figure 8c,d,h,i). The spinal process is short, rounded and not projecting beyond the posterior limits of the neural arches (Figure 8b,g). The neural canal is almost round (Figure 8a,d,f,I). The odontoid is attached to the anteroventral surface of the neural arches, with a dorsoanterior projection, that tapers anteriorly, ending in a rounded distal limit (Figure 8a,c,f,h). The ventral lamina of the neural canal represents a moderately developed keel, that almost reaches the condyle. No lateral foramina are visible in the centrum of the axis. Short transverse processes from the centrum are present (Figure 8a,d,f,i). The intercentra II and III are compressed laterally, fused and keel-shaped in lateral view, being medially separated by a concave area (Figure 8c,h).

3.4 | Rudimentary pelvic and hindlimb elements of *Epictia guayaquilensis* and *E. unicolor* (Figure 9)

Rudimentary pelvic and hindlimb elements are composed of the ilium, ischium, femur, and pubis. These elements are located ventral to the last two trunk vertebrae and the first cloacal vertebra and extend over three vertebrae (Figure 9a).

The **ilium** is rod-like and curved (distinctly more curved on the right side of the body in *E. guayaquilensis*) and represents the longest bone of the pelvic girdle. In *E. guayaquilensis* (Figure 9c), it is slightly longer than the pubis, while in *E. unicolor* (Figure 9b)—even though fused to it—it is about twice longer than the pubis. It is oriented lateroposteriorly to the body, and in *E. guayaquilensis* (Figure 9c) it is not in contact with any of the other bones of the pelvic girdle, while in *E. unicolor* (Figure 9b) it is fused to the pubis.

The **pubis** is rod-like, slightly curved and slightly tapered anteriorly. It represents the second longest and

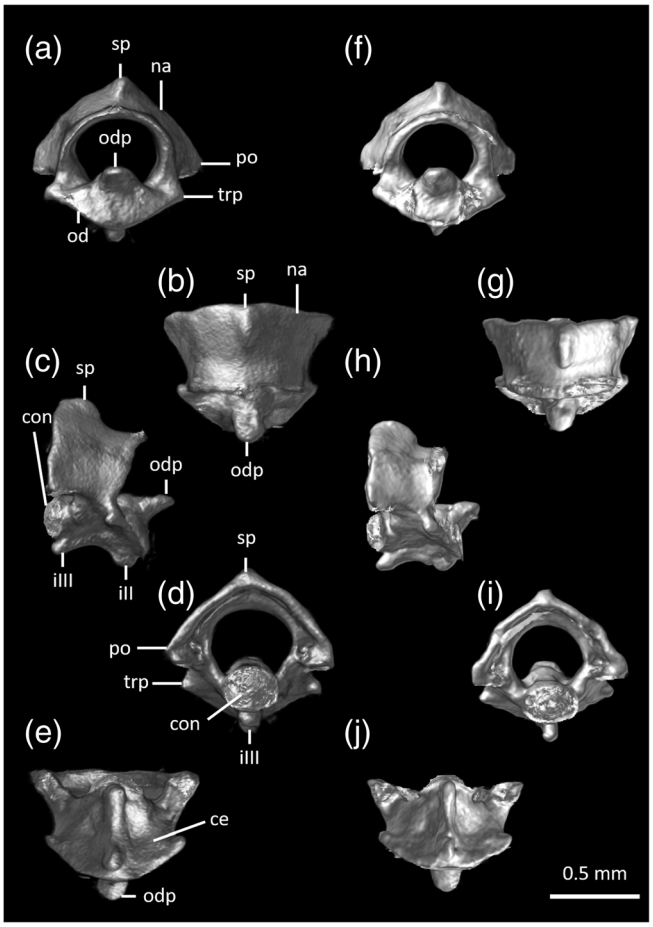

FIGURE 8 Three-dimensional reconstruction of the axis of the holotypes of *Epictia unicolor* (a–e, ZMH 8401) and *E. guayaquilensis* (f–j, ZMB 4508) in (a,f) anterior, (b,g) dorsal, (c,h) lateral, (d,i) posterior, and (e,j) ventral views. ce, centrum; con, condyle; iII, intercentrum II; iIII, intercentrum III; na, neural arches; od, odontoid; odp, odontoid process; po, postzygapophysis; sp, spinal process; trp, transverse process

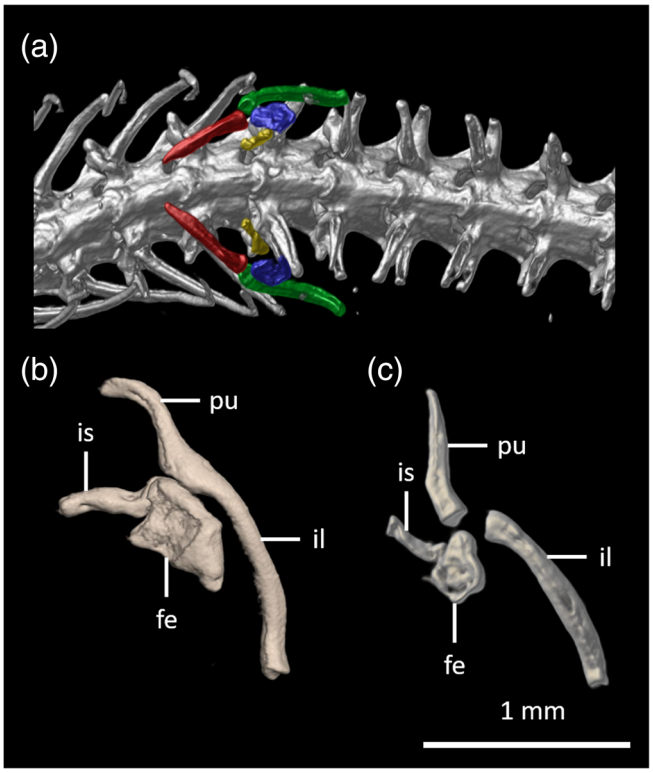

FIGURE 9 Three-dimensional reconstruction of the ventral view of the posterior region of the body of *E. guayaquilensis* (a, ZMB 4508), indicating the location and orientation of the femur (blue), ilium (green), ischium (yellow) and pubis (red), and the isolated pelvic and hindlimb elements of *Epictia unicolor* (b, ZMH 8401) and *E. guayaquilensis* (c, ZMB 4508) in lateral view. fe, femur; il, ilium; is, ischium; pu, pubis. The scale only refers to (b) and (c)

the anteriormost bone of the pelvic girdle (Figure 9a) and is only slightly shorter than the ilium. The pubis converges to its counterpart, but without contacting it (Figure 9a). In *E. guayaquilensis* it approaches the femur posteriorly but is still slightly separated from it and is also not in contact with the ilium and ischium (Figure 9c).

The **ischium** is rod-like, slightly curved and less than half the length of the pubis. It represents the most ventral bone of the pelvic girdle and is anteromedially oriented. It contacts (left ischium of *E. guayaquilensis* and both of *E. unicolor*; Figure 9b,c) or not (right ischium of *E. guayaquilensis*) the femur.

The **femur** is flattened and approximately round (*E. guayaquilensis*; Figure 9c) or trapezoidal (*E. unicolor*; Figure 9b) and located at the level between the last trunk vertebrae and the first cloacal vertebra (Figure 9a). An ossified claw-like element or femoral spur is not visible in the CT-images.

3.5 | Holotype redescription—*Epictia guayaquilensis* (Orejas-Miranda & Peters, 1970)—New combination (Figures 1, 3d–f, 4c,d, 5e–h, 6e–h, 7f–j, 8f–j, and 9b)

Leptotyphlops guayaquilensis Orejas-Miranda & Peters, 1970 [1969].

Tricheilostoma guayaquilensis—Hedges, Adalsteinsson & Branch *in* Adalsteinsson et al., 2009.

Trilepida guayaquilensis—Hedges, 2011.

Tricheilostoma guayaquilensis—Pinto & Fernandes, 2012.

Trilepida guayaquilensis—Wallach et al., 2014.

3.5.1 | Holotype

ZMB 4508, indeterminate sex, Ecuador, Guayas, Guayaquil (02°10′ S, 079°54′ W), C. Reiss.

3.5.2 | Diagnosis

Epictia guayaquilensis can be distinguished from other congeners by the following combination of characters: (a) truncate head in dorsal view and slightly acuminate in lateral view; (b) supraocular present and longer than frontal scale; (c) ocular subhexagonal with slightly rounded anterior margin at eye level and straight upper margin; (d) rostral subtriangular in dorsal view, reaching an imaginary transverse line between the anterior borders of the ocular scales; (e) lower margin of occipital scale does not reach upper margin of third supralabial; (f) temporal indistinct; (g) three supralabials (2 + 1); (h) four infralabials; (i) 253 middorsal scales; (j) 233 midventral scales; (k) 20 subcaudals; (l) fused caudals absent; (m) 12 midtail scale rows; (n) dorsal scales brown and ventral scales slightly lighter than dorsals in preservative.

3.5.3 | Redescription

Indeterminate sex, 170 mm total length (TL); 13 mm tail length (TAL); 3.5 mm midbody diameter (MB); 13.1 TL/TAL; 48.6 TL/MB; 4.4 mm head length; 2.4 mm head width; 1.6 mm head height; subcylindrical body, slightly larger at head and flattened in cloacal region; cervical constriction absent.

Head truncate in dorsal and ventral views, slighlty acuminate in lateral view; rostral subtriangular reaching imaginary transverse line between anterior borders of oculars; rostral contacting supra- and infranasals laterally and dorsally; nasal completely divided horizontally by oblique suture crossing nostril and descending posteriorly to contact first supralabial; nostril slightly elliptical, obliquely oriented and located in center of nasal suture; supranasal contacting rostral anteriorly, infranasal inferiorly, first and second supralabials, and ocular posteriorly, and frontal and supraocular dorsally; supranasal ventrally broader than dorsal margin of infranasal scale; upper lip border formed by rostral, infranasal, two anterior supralabials, ocular, and posterior supralabial; temporal indistinct in size from dorsal scales of lateral rows; three supralabials, first two anterior to ocular and one posterior (2 + 1); first supralabial subrectangular, almost twice as high as wide, reaching nostril but not eye level; second supralabial almost three times higher than wide, higher than first supralabial, surpassing level of nostril and reaching to level of center of eye; third supralabial triangular, as high as wide, surpassing level of nostril but not reaching eye level, its posterior margin in broad contact with temporal; ocular scale enlarged, subhexagonal, twice as high as wide, anterior border barely rounded at eye level, dorsal border straight, contacting posterior margins of supranasal and second supralabial anteriorly, parietal and third supralabial posteriorly, and supraocular dorsally; eye distinct, positioned in central area of upper part of ocular, located above nostril level; supraocular scale short, longer than wide and longer than frontal, between ocular and frontal, contacting supranasal and frontal anteriorly, postfrontal and ocular laterally, and parietal posteriorly; frontal and postfrontal subequal in size, hexagonal and weakly imbricate; frontal contacting rostral, supranasals, supraoculars, and postfrontal; postfrontal contacting frontal, supraoculars, parietals, and interparietal; interparietal and interoccipital longer than other middorsal scales, as long as

wide; interparietal contacting postfrontal, parietals, occipitals, and interoccipitals; interoccipital contacting interparietal, occipitals, first dorsal scale of vertebral row, and first pair of scales of dorsal paravertebral rows; parietal and occipital subequal, irregularly pentagonal; parietal lower margin contacting upper border of third supralabial, posterior margin contacting temporal, occipital, and interparietal, anterior border in contact with ocular, supraocular, and postfrontal; occipital shorter than parietal, its lower margin not reaching upper margin of third supralabial, separated from the latter by temporal; symphysial trapezoidal, anterior and posterior borders slightly straight and concave, respectively; four infralabials (six infralabials according to Orejas-Miranda and Peters (1970), who very likely counted the ventrally adjacent scales instead of the last infralabial, since the infralabial is obscured by the upper lip margin when the mouth is closed); fourth infralabial wider than others. Middorsal scales 253; midventral scales 233; scale rows around midbody 14, reducing to 12 rows at midtail; cloacal shield short, subcircular; subcaudals 20; fused caudals absent; terminal spine conical, very short. Dorsal scales homogeneous, cycloid, smooth, not imbricate, wider than long.

3.5.4 | Coloration of the holotype in preservative

Middorsal scales (i.e., seven longitudinal rows) brown or slightly reddish (also mentioned in original description). The remaining seven scale rows forming the ventral and lateral sides of the body are lighter in color than dorsal pattern; cloacal shield same color as ventral scales; terminal spine not pigmented.

3.5.5 | Remarks

Based on both osteology and external morphology, the species is assigned to the genus *Epictia*. *Epictia guayaquilensis* and all other *Epictia* spp. differ from *Trilepida* spp. by the presence of a ventral contact of the otooccipital bones, which excludes the basioccipital from the formation of the foramen magnum (vs. not in contact in *Trilepida*; Koch, Martins & Schweiger, 2019; Martins et al., 2021; Martins et al., 2019); by having paired supraoccipital bones (vs. fused; Koch et al., 2019; Martins et al., 2019; Martins et al., 2021) and by lacking fused caudal scales (vs. fused in *Trilepida*; Pinto, 2010). Several *Epictia* spp. exhibit a striped dorsal pattern (Adalsteinsson et al., 2009; Koch et al., 2019; Koch, Cruz & Cárdenas, 2016; Koch, Venegas & Böhme, 2015), in contrast to the invariable uniform dorsal coloration in all *Trilepida*. However, the striped pattern is not mentioned in the original description and is barely visible as the color of the specimen appears to be very faded due to preservation.

4 | DISCUSSION

When Adalsteinsson et al. (2009) divided the genus *Leptotyphlops* into 11 genera, they assigned the species "*L. guayaquilensis*" to the genus *Tricheilostoma* (now *Trilepida*, fide Hedges, 2011), based on external similarity to this species group previously described by Orejas-Miranda and Peters (1970) and mainly due to the presence of three supralabial scales. While some genera (e.g., *Mitophis*, *Rena*, *Trilepida*) have been assumed to have interspecific variation in the number of supralabial scales, Adalsteinsson et al. (2009) defined the genus *Epictia* in part by the presence of two supralabial scales. The species "*L. unicolor*" was not considered by Adalsteinsson et al. (2009), but later assigned to the genus *Epictia* without justification by Wallach et al. (2014), even though the species has four supralabial scales. However, our osteological examination shows that both "*Trilepida*" *guayaquilensis* and *E. unicolor* have the cranial features as seen in *Epictia* (see Koch et al., 2019; Martins, 2016; Martins et al., 2019), such as the presence of paired supraoccipital bones (fused in *Trilepida*; see Martins et al., 2021) and otooccipitals that are in ventral contact excluding the basioccipital from the foramen magnum (otooccipitals are not in ventral contact and basioccipital contributes to the formation of the foramen magnum in *Trilepida*; see Martins et al., 2021). Additionally, the absence of an intercentrum I of the atlas (contrasting with a well-developed intercentrum I present for example in *Rena* and *Trilepida*; see Martins et al., 2021) is in accordance with the pattern found in *Epictia*. Additionally, the presence of a posterior development of the quadrate (= posterior process in Martins, 2016) is also a characteristic of the genus *Epictia* which is not present in *Rena* (see Koch et al., 2019; Martins, 2016; Martins et al., 2019). Thus, we confirm the generic assignment of *E. unicolor* and propose a new combination, *Epictia guayaquilensis*.

We also provide a detailed redescription of the holotype of *E. guayaquilensis* and note that this species most likely belongs to *Epictia* rather than *Trilepida*, given the presence of paired supraoccipital bones, the fact that the otooccipitals are in ventral contact excluding the basioccipital from the foramen magnum, the lack of fused caudal scales, and the possible presence of a striped pattern (possibly faded by preservation; see "Remarks" in

the results section). Given the conserved nature of the external morphology of leptotyphlopids, osteological data (mostly from the skull) have aided in recent years in proposing diagnostic features for some genera within the Leptotyphlopidae (Martins et al., 2019; Martins et al., 2021). Martins et al. (2021) provide a combination of osteological characters that are exclusively shared by all 14 currently recognized species of *Trilepida*, supporting the taxonomic decision proposed herein. Thus, both the osteological data and morphological characters provided here contribute to confirm the reassessment of the generic status of *E. guayaquilensis* (previously mentioned in Pinto, 2010).

Epictia guayaquilensis and *E. unicolor* represent the only two species to date within the genus, which now contains 44 species (this study, Uetz et al., 2021; Koch et al., 2019; Martins et al., 2019), that have a divergent number of supralabial scales from two. In fact, variation in scalation not only occurs among different genera or species, but also within the same species or even bilaterally in the same individual (Curcio, Zaher & Rodrigues, 2002; Francisco, Pinto, & Fernandes, 2018; Pinto & Curcio, 2011; Wallach, 1996b). As previous authors have shown (e.g., Koch et al., 2019; Martins et al., 2021; Pinto et al., 2015), the intraspecific variability in osteological characters is reduced in skulls of leptotyphlopids and extremely reduced in the mandibular and post-cranial characters. Osteological modifications in these snakes, then, seem to be conserved and may represent a more confident feature for defining and distinguishing genera than scalation characters. We are currently working on a molecular study of the family Leptotyphlopidae. In the future, these genetic data may help to test the taxonomic boundaries proposed here.

Even though detailed descriptive osteological studies have increased in the past years—mostly due to the availability of HRXCT data—these kind of contributions are still scarce for *Epictia*, the most speciose genus amongst Leptotyphlopidae. Only a few general descriptions and/or illustrations (e.g., List, 1966) on the osteology of *Epictia* have been published, but the only comprehensive osteological description of a species is that of Koch et al. (2019). Thus, our study represents an increase in available data for *Epictia*, which also confirms some osteological characters that might be informative at a generic level, such as the ventral contact of the otooccipitals resulting in the exclusion of the basioccipital in the formation of the foramen magnum, a posterior elongation of the quadrate, paired supraoccipitals, paired nasals (although this might vary in the genus; List, 1966; Martins, 2016; Koch et al., 2019), and a reduced or absent intercentrum I. However, these observations are based on a relatively small number of species of *Epictia* and will be addressed in a future study with a larger taxonomic sampling. Our work shows once again how helpful the inclusion of anatomical data is in order to make more accurate systematic statements for leptotyphlopids.

ACKNOWLEDGMENTS

We are thankful to F. Tillack and M. Rödel (ZMB) and J. Hallermann (ZMH) for the loan of the holotypes. We are grateful to the editor J. D. Daza and three anonymous reviewers for important suggestions during the submission process that greatly improved our manuscript. Open Access funding enabled and organized by Projekt DEAL.

AUTHOR CONTRIBUTIONS

Claudia Koch: Conceptualization; data curation; investigation; methodology; project administration; resources; software; supervision; visualization; writing-original draft; writing-review & editing. **Angele Martins:** Conceptualization; investigation; methodology; visualization; writing-original draft; writing-review & editing. **Mitali Joshi:** Formal analysis; investigation. **Roberta Pinto:** Conceptualization; investigation; methodology; resources; visualization; writing-original draft; writing-review & editing. **Paulo Passos:** Writing-original draft; writing-review & editing.

ORCID

Claudia Koch https://orcid.org/0000-0002-7115-2816
Angele Martins https://orcid.org/0000-0002-0193-4011

REFERENCES

Abdeen, A. M., Abo-Taira, A. M., & Zaher, M. M. (1991a). Further studies on the ophidian cranial osteology: the skull of the Egyptian blind Snake *Leptotyphlops cairi* (family Leptotyphlopidae). I. The cranium. A. the median dorsal bones, bones of the upper jaw, circumorbital series and occipital ring. *Journal of the Egyptian-German Society of Zoology (Giza)*, *5*(5), 417–437.

Abdeen, A. M., Abo-Taira, A. M., & Zaher, M. M. (1991b). Further studies on the ophidian cranial osteology: The skull of the Egyptian blind Snake *Leptotyphlops cairi* (family Leptotyphlopidae). I. the cranium. B. the otic capsule, palate and temporal bones. *Journal of the Egyptian-German Society of Zoology (Giza)*, *5*(5), 439–455.

Abdeen, A. M., Abo-Taira, A. M., & Zaher, M. M. (1991c). Further studies on the ophidian cranial osteology: The skull of the Egyptian blind Snake *Leptotyphlops cairi* (family Leptotyphlopidae). II. The lower jaw and the hyoid apparatus. *Journal of the Egyptian-German Society of Zoology (Giza)*, *5*(5), 457–467.

Adalsteinsson, S. A., Branch, W. R., Trape, S., Vitt, L. J., & Hedges, S. B. (2009). Molecular phylogeny, classification, and biogeography of snakes of the family Leptotyphlopidae (Reptilia, Squamata). *Zootaxa*, *2244*, 1–50.

Boundy, J., & Wallach, V. (2008). The identity of the leptotyphlopid snake *Glauconia unicolor*, Werner, 1913 (Squamata: Serpentes:

Leptotyphlopidae). *Mitteilungen Aus Dem Hamburgischen Zoologischen Museum Und Institut*, *105*, 53–56.

Broadley, D. G. (1999). A new species of worm snake from Ethiopia (Serpentes: Leptotyphlopidae). *Arnoldia Zimbabwe*, *10*, 141–144.

Broadley, D. G. (2004). A specimen of *Leptotyphlops bicolor* (Jan) from Ghana with a "subocular" (Serpentes; Leptotyphlopidae), with a note on the skull of this species. *African Journal of Herpetology*, *53*(1), 87–89.

Broadley, D. G., & Broadley, S. (1999). A review of the African worm snakes from south of latitude 12°S (Serpentes: Leptotyphlopidae). *Syntarsus*, *5*, 1–36.

Broadley, D. G., & Wallach, V. (1997). A review of the genus *Leptotyphlops* (Serpentes: Leptotyphlopidae) in Kwazulu–Natal, with the description of a new forest–dwelling species. *Durban Museum Novitates*, *22*, 37–42.

Broadley, D. G., & Wallach, V. (2007). A revision of the genus *Leptotyphlops* in northeastern Africa and southwestern Arabia (Serpentes: Leptotyphlopidae). *Zootaxa*, *1408*, 1–78.

Brock, G. T. (1932). The skull of *Leptotyphlops* (*Glauconia nigricans*). *Anatomischer Anzeiger*, *73*, 199–204.

Cisneros-Heredia, D. F. (2008). Reptilia, Squamata, Leptotyphlopidae, *Leptotyphlops*, Ecuador: Re-evaluation of the species cited for the country. *Check List*, *4*(2), 178–181.

Cundall, D., & Irish, F. (2008). The snake skull. In C. Gans & T. S. Parsons (Eds.), *Biology of the Reptilia* (Vol. 20, pp. 349–692). London: Academic Press.

Curcio FF. 2003. Osteologia craniana comparada e filogenia da família Anomalepididae Taylor, 1939 (Serpentes, Scolecophidia). Ph.D. thesis, Sao Paulo, Universidade de Sao Paulo.

Curcio, F. F., Zaher, H., & Rodrigues, M. T. (2002). Rediscovery of the blind-snake *Leptotyphlops brasiliensis* Laurent, 1949 (Serpentes, Leptotyphlopidae) in the wild. *Phyllomedusa*, *1*, 101–104.

Duerden, J. E., & Essex, R. (1923). The pelvic girdle in the snake *Glauconia*. *South African Journal of Science*, *20*, 354–356.

Duméril, A. M. C., & Bibron, G. (1844). *Erpétologie Générale ou Histoire Naturelle Complète des Reptiles* (Vol. 6). Paris: Librairie Encyclopédique de Roret.

Essex, R. (1927). Studies in reptilian degeneration. *Proceedings of the Zoological Society of London*, *4*, 879–945.

Fabrezi, M., Marcus, A., & Scrocchi, G. (1985). Contribución al conocimento de los Leptotyphlopidae de Argentina I. *Leptotyphlops weyrauchi* y *Leptotyphlops albipuncta*. *Cuadernos de Herpetologia*, *1*, 1–20.

FitzSimons, V. F. M. (1962). *Snakes of southern Africa*. London: MacDonald.

Francisco, B., Pinto, R. R., & Fernandes, D. (2018). Taxonomic notes ond the genus *Siagonodon* Peters, 1881, with a report on morphological variation in *Siagonodon cupinensis* (Bailey and Crvalho, 1946) (Serpentes, Leptotyphlopidae). *Copeia*, *106*, 321–328.

Haas, G. (1930). Über das Kopfskelett und die Kaumuskulatur der Typhlopiden und Glauconiiden. *Zoologische Jahrbücher. Abteilung für Anatomie und Ontogenie der Tiere*, *52*, 1–94.

Haas, G. (1931). Über die Morphologie der Kiefermuskulatur und die Schädelmechanik einiger Schlangen. *Zoologische Jahrbücher der Anatomie*, *54*, 33–416.

Haas, G. (1959). Bemerkungen über die Anatomie des Kopfes und des Schädels der Leptotyphlopidae (Ophidia), speziell von *L. macrorhynchus* Jan. *Vierteljahresschrift der Naturforschenden Gesellschaft Zürich*, *104*, 90–104.

Haas, G. (1964). Anatomical observations on the head of *Liotyphlops albirostris* (Typhlopidae Ophidia). *Acta Zoologica*, *45*, 1–62.

Hahn, D. E. (1978). Brief review of the genus *Leptotyphlops* (Reptilia, Serpentes, Leptotyphlopidae) of Asia, with description of a new species. *Journal of Herpetology*, *12*, 477–489.

Hardaway, T. E., & Williams, K. L. (1976). Costal cartilages in snakes and their phylogenetic significance. *Herpetologica*, *32*, 378–387.

Hedges, S. B. (2011). The type species of the threadsnake genus *Tricheilostoma* Jan revisited (Squamata, Leptotyphlopidae). *Zootaxa*, *3027*, 63–64.

Holman, J. A. (2000). *Fossil snakes of North America: Origin, evolution, distribution, paleoecology*. Indiana: Indiana University Press.

Kley, N. J. (2001). Prey transport mechanisms in blindsnakes and the evolution of unilateral feeding systems in snakes. *American Zoologist*, *41*, 1321–1337.

Kley, N. J. (2006). Morphology of the lower jaw and Suspensorium in the Texas Blindsnake, *Leptotyphlops dulcis* (Scolecophidia: Leptotyphlopidae). *Journal of Morphology*, *267*, 494–515.

Koch, C., Venegas, P., & Böhme, W. (2015). Three new endemic species of Gray, 1845 (Serpentes: Leptotyphlopidae) from the dry forest of northwestern Peru. *Zootaxa*, *3964*, 228–244.

Koch, C., Cruz, R., & Cárdenas, H. (2016). Two new endemic species of *Epictia* Gray, 1845 (Serpentes: Leptotyphlopidae) from northern Peru. *Zootaxa*, *4150*, 101–122.

Koch, C., Martins, A. R., & Schweiger, S. (2019). A century of waiting: Description of a new *Epictia* gray, 1845 (Serpentes: Leptotyphlopidae) based on specimens housed for more than 100years in the collection of the Natural History Museum Vienna (NMW). *PeerJ*. *7*, 1–37. https://doi.org/10.7717/peerj.7411

List, J. C. (1966). Comparative osteology of the snake families Typhlopidae and Leptotyphlopidae. *Illinois Biological Monographs*, *36*, 1–112.

Martins AR. 2016. Morfologia interna comparada de representantes da subfamília Epictinae (Serpentes, Scolecophidia, Leptotyphlopidae). Ph.D. Thesis, Universidade de Rio de Janeiro.

Martins, A. R., Koch, C., Pinto, R. R., Folly, M., Fouquet, A., & Passos, P. (2019). From the inside out: Discovery of a new genus of threadsnakes based on anatomical and molecular data, with discussion of the leptotyphlopid hemipenial morphology. *Journal of Zoological Systematics and Evolutionary Research*, *57*(4), 840–863. https://doi.org/10.1111/jzs.12316

Martins, A. R., Passos, P., & Pinto, R. R. (2019). Moving beyond the surface: Comparative head and neck myology of threadsnakes (Epictinae, Leptotyphlopidae, Serpentes), with comments on the 'scolecophidian' muscular system. *PLoS One*, *14*, e0219661.

Martins, A. R., Koch, C., Joshi, M., Pinto, R. R., & Passos, P. (2021). Picking up the threads: Descriptive osteology and associated cartilaginous elements of the genus *Trilepida* Hedges, 2011 (Serpentes, Leptotyphlopidae, Epictinae) with the proposition of an osteological diagnosis for the genus. *Anatomical Record*.

McDiarmid, R. W., Campbell, J. A., & Touré, T. (1999). *Snakes species of the world. A taxonomic and geographic reference. Volume 1*. Washington, DC.: The herpetologists' league.

McDowell, S. B., & Bogert, C. M. (1954). The systematic position of *Lanthanotus* and the affinities of the anguinomorphan lizards. *Bulletin of the American Museum of Natural History*, *105*, 1–142.

Natera Mumaw, M., Esqueda González, L. F., & Castelaín, F. M. (2015). *Atlas serpientes de Venezuela: una visión actual de su diversidad*. Santiago de Chile: Fundación Biogeos, Asociación Venezolana de Herpetologia, Fundación Ecologica sin Fronteras y Serpentario.com.

Orejas-Miranda, B. R. (1967). El genero "*Leptotyphlops*" en la región Amazónica. *Atas do Simpósio sôbre a Biota Amazonica*, *5*, 421–442.

Orejas-Miranda, B. R., & Peters, J. A. (1970). Eine neue Schlankblindschlange (Serpentes: Leptotyphlopidae) aus Ecuador. *Mitt Zool Mus Berlin*, *46*, 439–441.

Orejas-Miranda, B. R., Roux-Estève, M. R., & Guibé, J. (1970). Un nouveau genre de Leptotyphlopides (Ophidia) *Rhinoleptus koniagui* (Villiers). *Comunicaciones Zoologicas del Museo de Historia Natural de Montevideo*, *10*, 1–4.

Parker, H. W., & Grandison, A. G. C. (1977). *Snakes: A natural history*. London and Ithaca, NY: British Museum (Natural History) and Cornell University Press.

Peters, J. A. (1970). Catalogue of the Neotropical Squamata: Part 1. Snakes. *Bulletin of the United States National Museum*, *297*, 1–347.

Pinto RR. 2010. Revisão sistemática da Subtribo Renina (serpentes: Leptotyphlopidae). Unpublished Thesis. Museu Nacional: Rio de Janeiro.

Pinto, R. R., & Curcio, F. (2011). On the generic identity of *Siagonodon brasiliensis*, with the description of a new leptotyphlopid from Central Brazil (Serpentes: Leptotyphlopidae). *Copeia*, *2011*, 53–63.

Pinto, R. R., & Fernandes, R. (2012). A new blind snake species of the genus *Tricheilostoma* from Espinhaço range, Brazil and taxonomic status of *Rena dimidiata* (Jan,1861) (Serpentes: Epictinae: Leptotyphlopidae). *Copeia*, *2012*, 37–48.

Pinto, R. R., Passos, P., Portilla, J., Arredondo, J., & Fernandes, R. (2010). Taxonomy of the threadsnakes of the tribe Epictini (Squamata:Serpentes:Leptotyphlopidae) in Colombia. *Zootaxa*, *2724*, 1–28.

Pinto, R. R., Martins, A. R., Curcio, F. F., & De O. Ramos, L. (2015). Osteology and cartilaginous elements of *Trilepida salgueiroi* (Amaral, 1954) (Scolecophidia: Leptotyphlopidae). *The Anatomical Record*, *298*, 1722–1747.

Rieppel, O. (1979). The braincase of *Typhlops* and *Leptotyphlops* (Reptilia: Serpentes). *Zoological Journal of the Linnean Society*, *65*, 161–176.

Rieppel, O., Kley, N. J., & Maisano, J. A. (2009). Morphology of the skull of the white-nosed blindsnake, *Liotyphlops albirostris* (Scolecophidia: Anomalepididae). *Journal of Morphology*, *270*, 536–557.

Romer, A. S. (1956). *Osteology of the reptiles*. Chicago: University of Chicago Press.

Salazar-Valenzuela, D., Martins, A., Amador-Oyola, L., & Torres-Carvajal, O. (2015). A new species and country record of threadsnakes (Serpentes: Leptotyphlopidae: Epictinae) from northern Ecuador. *Amphibian & Reptile Conservation*, *8*(1), 107–120.

Thomas, R. (1965). *The genus Leptotyphlops in the West Indies with the description of a new species from Hispaniola (Serpentes, Leptotyphlopidae)* (pp. 1–12). Museum of Comparative Zoology: Breviora.

Thomas, R., McDiarmid, R. W., & Thompson, F. G. (1985). Three new species of thread snakes (Serpentes, Leptotyphlopidae) from Hispaniola. *Proceedings of the Biological Society of Washington*, *98*, 204–220.

Uetz P, Freed P, Hosek, J. 2021. The Reptile Database. Retrieved from http://www.reptile-database.org.

Wallach, V. (1996a). *Leptotyphlops drewesi* n. sp., a worm snake from Central Kenya (Serpentes: Leptotyphlopidae). *Journal of African Zoology*, *110*, 425–431.

Wallach, V. (1996b). Notes and corrections on two scolecophidians: *Rhamphotyphlops albiceps* and *Leptotyphlops brasiliensis*. *Herpetological Review*, *27*, 10.

Wallach, V. (2003). Scolecophidia miscellanea. *Hamadryad*, *27*, 222–240.

Wallach, V., & Hahn, D. E. (1997). *Leptotyphlops broadleyi*, a new species of worm snake from Cote d'Ivoire (Serpentes: Leptotyphlopidae). *African Journal of Herpetology*, *46*, 103–109.

Wallach, V., Williams, K. L., & Boundy, J. (2014). *Snakes of the world: A catalogue of living and extinct species*. Florida: CRC Press.

Werner, F. (1913). Neue oder seltene Reptilien und Frösche des Naturhistorischen Museums in Hamburg. *Mitteilungen aus den Hamburgischen Zoologischen Museum und Institut*, *30*, 1–51.

How to cite this article: Koch, C., Martins, A., Joshi, M., Pinto, R. R., & Passos, P. (2021). Osteology of the enigmatic threadsnake species *Epictia unicolor* and *Trilepida guayaquilensis* (Serpentes, Leptotyphlopidae) with generic insights. *The Anatomical Record*, 1–15. https://doi.org/10.1002/ar.24676